Supplementary information

Potential of Na_3AlF_6 as solid electrolyte for all-solid-state Na batteries

Reona Miyazaki[a], En Yagi [b], Yusuke Harazono [b], Natsuki Ito [b], Toshihiro Yoshida [b] and Takahiro Tomita [b]*

a. Department of Physical Science and Engineering, Graduate School of Engineering, Nagoya Institute of Technology, Aichi 466-8555, Japan

b. NGK INSULATORS, LTD., 2-56 Suda-cho, Mizuho, Nagoya 467-8530, Japan

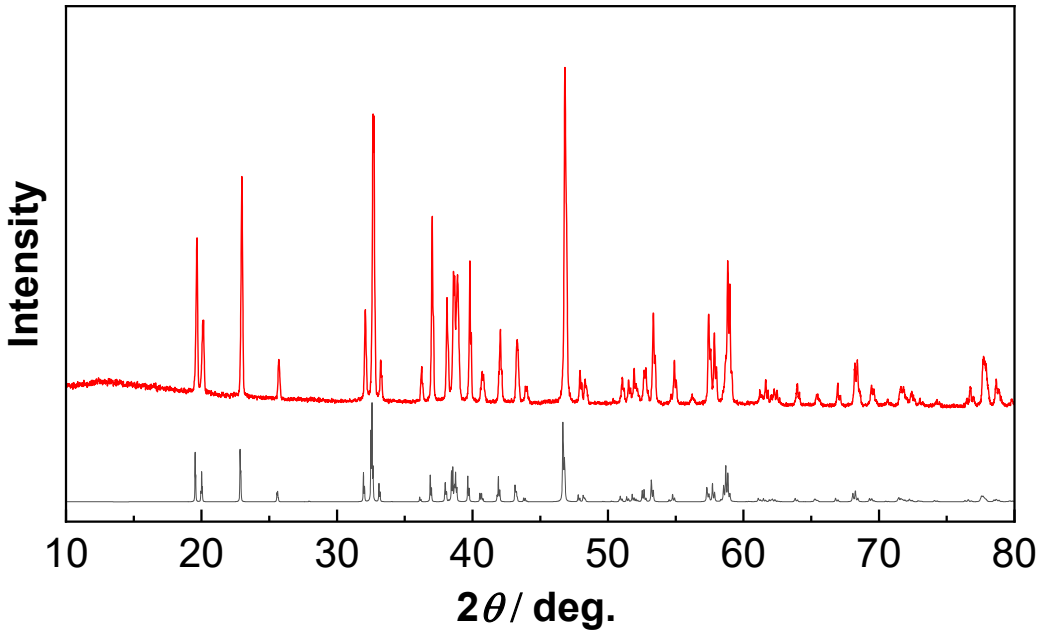

Figure S1 (Top) XRD pattern of as-prepared Na_3AlF_6 and (Bottom) theoretical pattern for Na_3AlF_6 ($P2_1/n$).

Figure S1 represents the XRD pattern of Na_3AlF_6 prepared by melting at 1050°C for 10 min. Diffraction pattern was almost coincidence with that for ideal Na_3AlF_6 ($P2_1/n$). Theoretical pattern was simulated by using VESTA software [*J. Appl. Cryst.* (2011). **44**, 1272-1276].

As shown in Figure S2(a), MSD of Na^+ was still below $0.3A^2$ after 1000ps for stoichiometric Na_3AlF_6. The continuous increase of MSD was not confirmed by temperature rising, indicating that Na^+ conductivity of Na_3AlF_6 is extremely low without Na^+ vacancies. On the other hand, slight increase in MSD for F^- was confirmed (Figure S2(c)). The MSF of F^- can be attributable to the hopping of F^- around AlF_6^{3-}. As shown in Figure S2(d), F^- ions exchanged the vertex of AlF_6^{3-} octahedra with time. Such a local hopping of F^- does not contribute for the long-range diffusion. Hence, in the stoichiometric Na_3AlF_6, neither Na^+ nor F^- contribute for the ion conduction and the observed ion dynamics is the F^- hopping around AlF_6^{3-}.

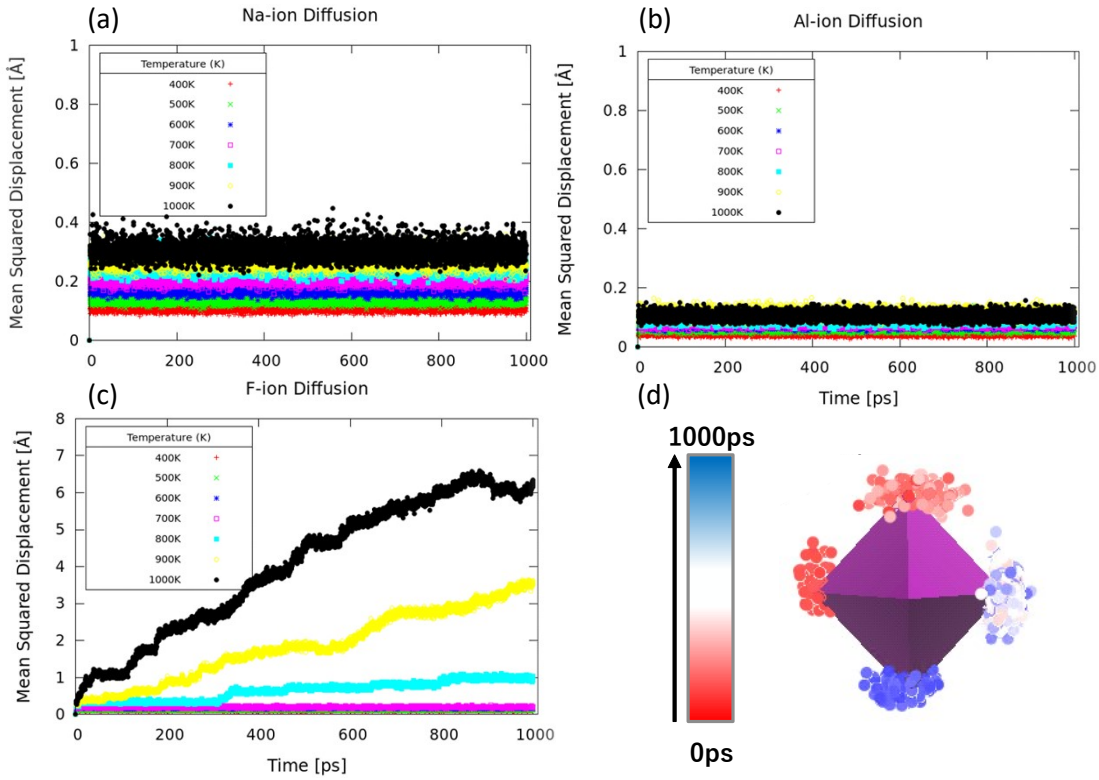

Figure S2(a)-(c): MSDs calculated between 400-1000K for stoichiometric Na_3AlF_6 without vacancies. (d): Trajectory mapping of F^- around AlF_6^{3-} octahedra at 1000K.

The default monoclinic structure ($P2_1/n$) includes 456 atoms (Na = 120, Al = 24, Si = 24, F = 288). The calculated MSD of Na^+ at 700-1000 K (Figures S3(a)-(d)) increased with temperature, indicating long-range hopping of Na^+ in monoclinic Na_3AlF_6. On the other hand, the MDS of F^- remained unchanged above 60 ps. The MSD of F^- was not further increased until 1000 K, with a maximum value of ~6 Å^2. Hence, although the F^- motion was facilitated, F^- ions did not contribute to the long-range diffusion for the case that F^- vacancies are not included in $Na_3AlF_6 \cdot Na_2SiF_6$.

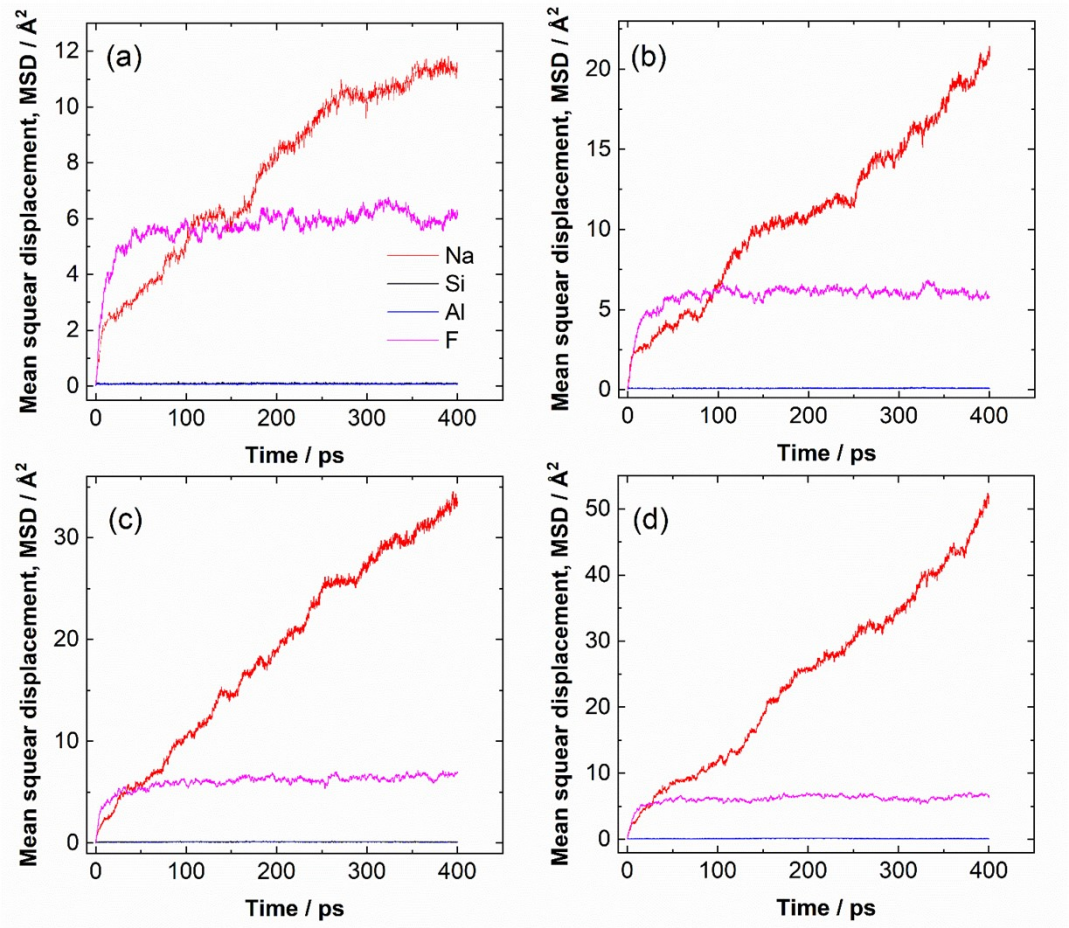

Figure S3: MSD of Na(red), Al (blue), Si (black) and F (magenta) of $Na_3AlF_6 \cdot Na_2SiF_6$ without F^- vacancies at (a) 700K, (b) 800K, (c) 900K, and (d) 1000K. Note that MSDs of Si are almost overlapped with those of Al.

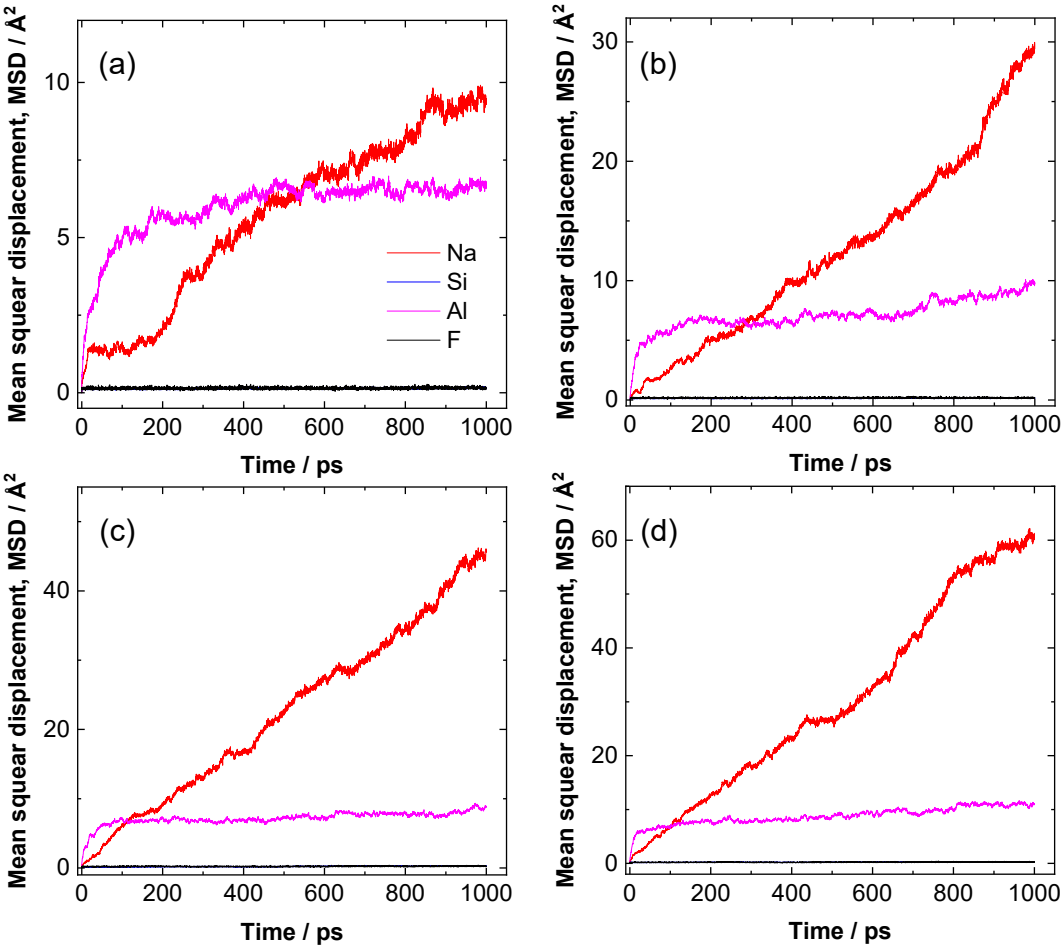

Figure S4: MSD of Na(red), Al (blue), Si (black) and F (magenta) of Na_3AlF_6-Na_2SiF_6 (Si 25 mol%) at (a) 700K, (b) 800K, (c) 900K, and (d) 1000K. F^- vacancies were included in a similar manner with the simulation of $Na_3AlF_6 \cdot Na_2SiF_6$ (Si 50 mol%). Note that MSDs of Si are almost overlapped with those of Al.

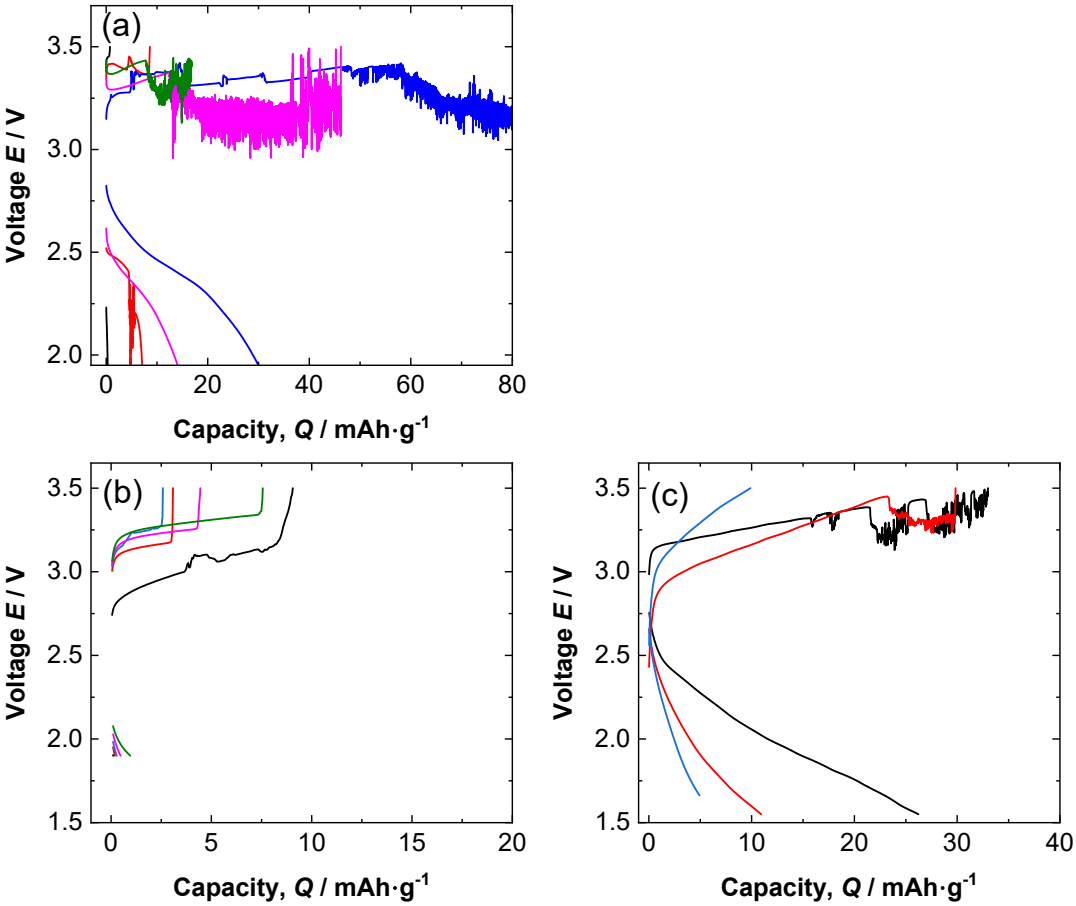

Figure S5: Charge-discharge curves of the cell using (a) Na_3Sn and (b)(c) $NaSn_3$ alloy anodes. Black, red, blue and green lines represent the results of first, second, third and fourth cycles, respectively. The measurement current was 50 μA for (a) and (b) while the charge-discharge rate was decreased to 20 μA for (c)

The cell fabrication procedures are same with those of Na/$NaCrO_2$ cell excepting that the Na-Sn alloy is used as anode. After pressing the solid electrolyte and $NaCrO_2$ composite together, a given molar ratio of Na and Sn tip was placed on the pellet opposite from $NaCrO_2$ composite side. The cell was finally screwed at 6 Nm. The charge-discharge measurement was performed at 60°C. Figure S5(a) represents the charge-discharge results using Na_3Sn anode. Charge-discharge current was 50 μA. The cell underwent the voltage disturbance during charging, which was more significant than that of Na/$NaCrO_2$ cell (Figure 8). Figure S5(b) and (c) are the results for the cell with $NaSn_3$ anode. The capacities were drastically decreased under 50 μA (Figure S5(b)). When the charge-discharge current was decreased to 20 μA, capacities were rather increased. However, the

voltage disturbance was still observed during charging. Finally, the capacities were decreased to 10 mAh/g at 3rd cycle.